Materials Letters 119 (2014) 100–103

Contents lists available at ScienceDirect

Materials Letters

journal homepage: www.elsevier.com/locate/matlet

Facile synthesis of Cu–In–Zn–S alloyed nanocrystals with temperature-dependent photoluminescence spectra

Zeshan Leng, Liang Huang, Feng Shao, Zhicheng Lv, Tingting Li, Xiaoxu Gu, Heyou Han *

College of Science, State Key Laboratory of Agricultural Microbiology, Huazhong Agricultural University, Wuhan 430070, China

ARTICLE INFO

Article history:
Received 18 November 2013
Accepted 28 December 2013
Available online 6 January 2014

Keywords:
Nanocrystalline materials
Luminescence
Structural

ABSTRACT

A facile strategy has been developed for the synthesis of highly luminescent Cu–In–Zn–S (CIZS) quaternary alloyed nanocrystals. The photoluminescence emission wavelength could be tuned from 520 nm to 700 nm only by varying the diffusion temperature, and an up to 76% of quantum yield was obtained after coating with the ZnS shell. The results of high resolution transmission electron microscopy and X-ray diffraction demonstrated the small particle size (2.5 nm), high crystallinity and alloyed structure of all the CIZS NCs. The photoluminescence mechanism of CIZS NCs before and after ZnS coating was also investigated by analyzing the PL decay curves.

1. Introduction

$CuInS_2$ (CIS) has been intensively investigated due to its optical and photovoltaic properties [1–3]. However, the photoluminescence quantum yield (PLQY) is always low (about 5%), which is not suitable for special applications where strong fluorescence is required. As an alternative, quaternary Cu–In–Zn–S NCs have received considerable attention [4–6]. Apart from the highly improved emission efficiency, the optical spectrum of CIZS can be varied in the whole visible region through alloying CIS (E_g=1.5 eV) with ZnS (E_g=3.7 eV), which is of special interest in both solar energy conversion and fluorescence emission. An early example was reported by Nakamura et al. through thermolysis of zinc dithiocarbamate with copper iodide and indium iodide in oleylamine solution [4]. The PL wavelength of $CuInS_2$–ZnS NCs was controllable from 570 to 800 nm. Recently, Zhang et al. synthesized CIZS alloyed NCs via a reaction between the acetate salts and elemental sulfur in a noncoordinating solvent and the PLQY increased to 56% [7]. However, their method is complicated, requiring the pre-treatment of all the metal precursors. Moreover, most of CIZS NCs were synthesized directly by heating in one-pot, which is a challenge for balancing the relative chemical reactivity of cationic precursors. Thus, much effort has been focused on seeking a simple method to prepare CIZS NCs with controlled compositions and relative chemical reactivity of cationic precursors.

In this paper, highly luminescent CIZS alloyed NCs were synthesized using commercial precursors by a stepwise approach. Only by changing the diffusion temperature, a variety of CIZS NCs with different band gaps could be obtained. The as-prepared NCs showed high quality luminescence properties and high crystallinity with narrow size distribution. This simple method has the potential to control the relative chemical reactivity of cationic precursors and compositions of the resulting CIZS NCs.

2. Experimental

In a typical procedure, 4.5 mg of copper (II) acetate, 29.2 mg of indium acetate, 0.5 ml of n-dodecanethiol, and 5 ml of 1-octadecene (ODE) were loaded into a three-necked flask. After being degassed and purged with argon, the mixture was heated to 100 °C for 10 min, followed by increasing to 230 °C for another 30 min. Subsequently, a solution of 36.7 mg of zinc acetate dissolved in 2 ml of oleylamine was injected into the flask, followed by heating under several temperatures for 30 min. For the ZnS shell overcoating, a stock solution of 91.7 mg of zinc acetate dissolved in 2 ml of TBP was added dropwise to the CIZS solution at 210 °C, followed by maintaining for 30 min. After cooled to room temperature, the NCs were isolated by adding ethanol and re-dispersed in toluene.

X-ray diffraction (XRD) measurement was performed by a Rigaku D/MAX-rA diffractometer with Cu Kα radiation. Transmission electron microscopy (TEM) images were recorded by JEM2010 with an EDS attachment operating at an accelerating voltage of 200 kV. X-ray photoelectron spectroscopy (XPS) measurements were performed with a Kratos XSAM800 system using Mg Kα source. UV–vis absorption spectra were recorded by a Nicolet Evolution 300 spectrometer. PL spectra and decay curves were measured with an Edinburgh FLS920 spectrometer (λ_{ex}=390 nm). The PLQYs were determined using Rhodamine 6G in ethanol as a standard (PLQY=95%).

* Corresponding author. Tel.: +86 27 87288246; fax: +86 27 87282133.
E-mail address: hyhan@mail.hzau.edu.cn (H. Han).

0167-577X/$ - see front matter © 2014 Elsevier B.V. All rights reserved.
http://dx.doi.org/10.1016/j.matlet.2013.12.109

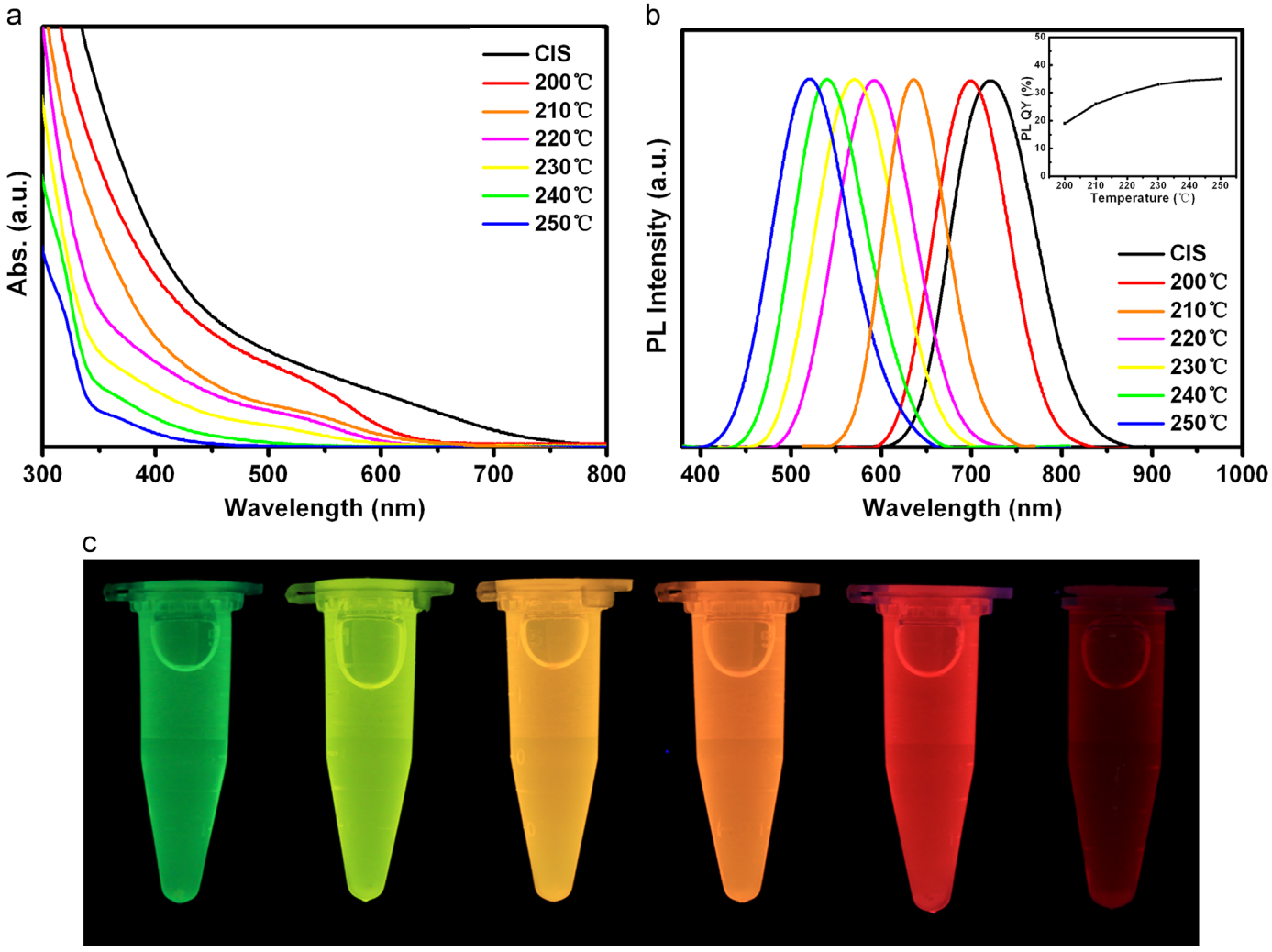

Fig. 1. Absorption, PL spectra, PLQY (inset) and photograph of CIZS NCs under different diffusion temperatures.

3. Results and discussion

Fig. 1a and b presents the absorption and emission spectra of CIZS NCs, respectively. The absorption band edges underwent a substantial blue-shift with an increase in diffusion temperature. HRTEM observation (Fig. S1) indicated that all of CIZS samples had almost the same particle size, excluding the size effect on the shift of band edges. Thus, the shift of absorption band edges can be attributed to variation in the composition of CIZS NCs (Table S1). Also, the corresponding PL emission peaks were tunable from 700 nm to 520 nm, implying the nature of introduction of Zn into CIS NCs. With the continuous heating after zinc precursor injection, CIS–ZnS alloyed structure would be formed by incorporating the wider band gap ZnS into the narrower band gap CIS. The reactivity of Zn^{2+} will be improved with increasing temperature, leading to an increasing amount of Zn^{2+} diffused [8]. Accordingly, the level of band gap formed will be enlarged and the greater blue-shift will occur. It is worth noting that the whole PL spectra maintained a single peak rather than multiple peaks compared to the previous reports [7,9], indicating the success in controlling the relative chemical reactivity of cationic precursors and preventing independent nucleation with this facile strategy.

Fig. 1c shows the picture of CIZS samples under a 365 nm UV lamp. As can be seen obviously, the emission colors ranged from deep red to green. Also, the PLQY of resulting NCs varied from 19% to 35% with increase in diffusion temperature. The enhanced PL

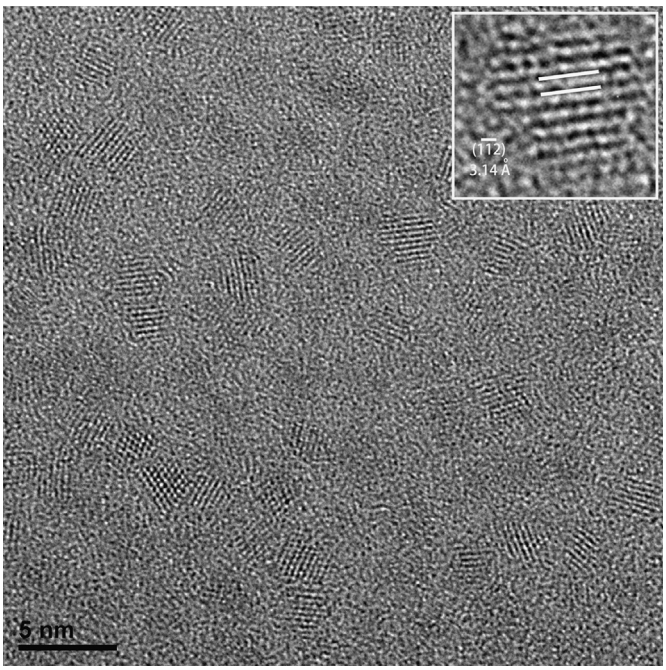

Fig. 2. HRTEM image of CIZS NCs prepared with the diffusion temperature of 230 °C.

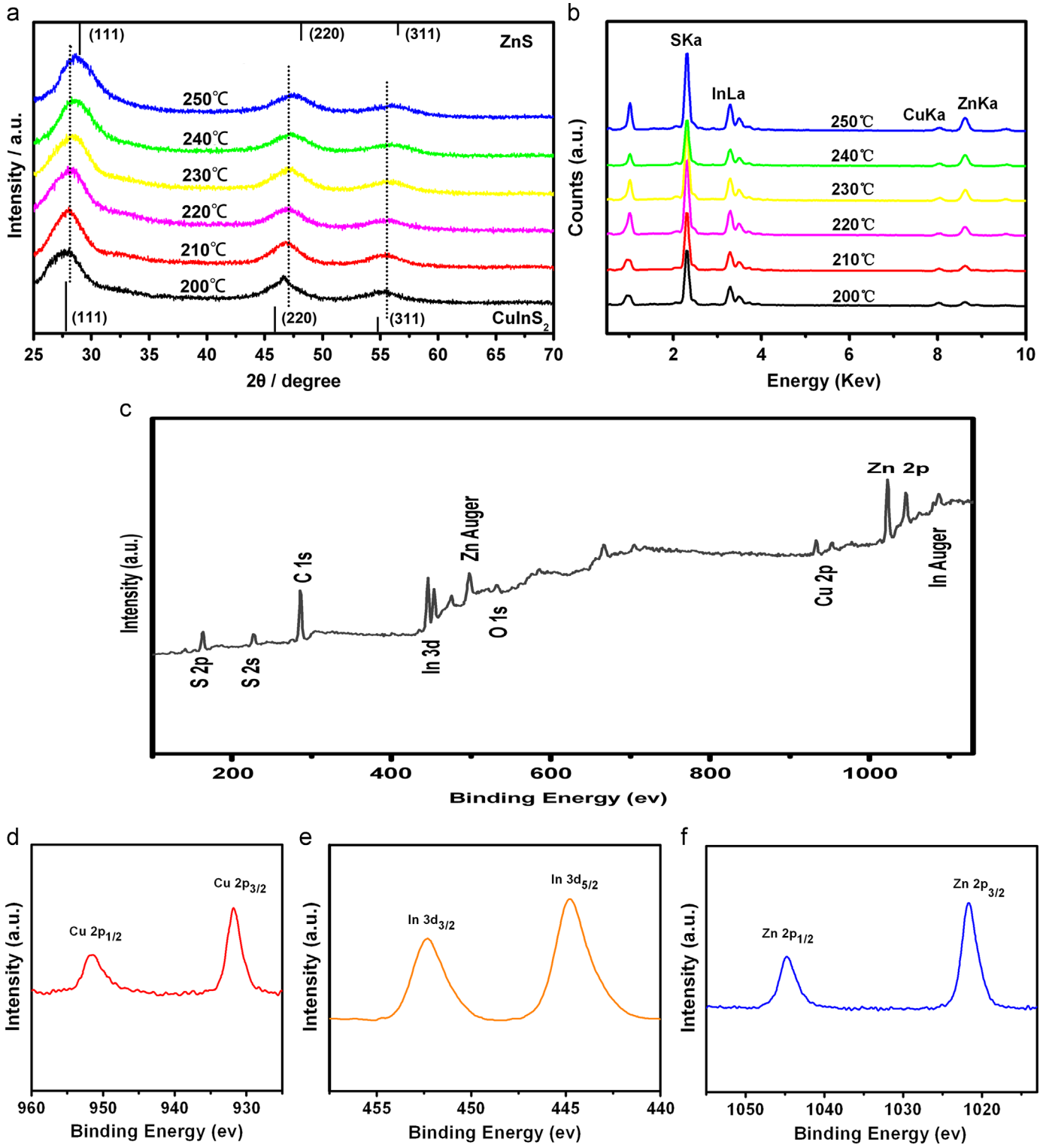

Fig. 3. XRD patterns (a), EDS spectra (b), XPS survey spectrum (c), the XPS spectrum of Cu 2p (d), the XPS spectrum of In 3d (e), the XPS spectrum of Zn 2p and (f) the XPS spectrum of CIZS NCs.

intensity, compared to pure $CuInS_2$ NCs, was ascribed to an increase in the population of donor–acceptor defects which were required for DAP recombination through highly off-stoichiometric ([Cu]/[In] molar ratio of 1:4) effects [10]. Moreover, the alloying ZnS component introduced more lattice dislocation into the system and thus hardening the crystal structure [11]. As a result, more Zn^{2+} being introduced exhibited much higher quantum yield.

The HRTEM image illustrated the nearly spherical and monodispersed NCs (Fig. 2), implying high nanocrystal quality. Moreover, the continuous lattice fringes throughout the whole particle revealed the high crystallinity with a d-spacing of 3.14 Å. In spite of the difference in diffusion temperature, the sizes of all the CIZS NCs were about 2.5 nm (Fig. S1).

Fig. 3a shows the XRD patterns, demonstrating the crystallinity and structure of CIZS NCs. A similar zinc blend structure could be

observed in all NCs and the diffraction pattern peaks shifted toward higher angles with increasing diffusion temperature. All the three characteristic peaks were located between the distinct diffraction peaks of $CuInS_2$ (JCPDS 47-1372) and ZnS (JCPDS 65-9585), indicating the introduction of Zn^{2+} ions and the formation of Cu–In–Zn–S alloyed structure.

The introduction of Zn into CIS was further supported by EDS analysis and XPS result. As shown in Fig. 3b, Zn element is detected in all of the CIZS samples. With increase in diffusion temperature, the mole fraction of Zn (Zn/(Cu+ In+ Zn)) increased from 28.54% to 54.65% systematically (Table S1). It was clearly shown that the Zn contents were increased effectively with increasing diffusion temperature. The prominent peaks of Zn 2p were obtained from XPS result (Fig. 3c), confirming the presence of Zn atoms in CIZS NCs, and the calculated atomic ratio obtained from the XPS spectra was in line with the EDS result (Table S2). In addition, the $2p_{3/2}$(931.8 eV) and $2p_{1/2}$ (951.6 eV) peaks of Cu, the $3d_{5/2}$(444.8 eV) and $3d_{3/2}$(452.3 eV) peaks of In, and the $2p_{3/2}$ (1021.7 eV) and $2p_{1/2}$ (1044.8 eV) peaks of Zn indicated that their valence states were +1, +3, and +2, respectively.

As reported in the previous studies [12,13], the introduction of Zn into CIS was achieved by partial cation exchange of Cu^+ or In^{3+} with Zn^{2+}. However, compared to CIS, the extent of blue-shift for CIZS reported in those studies was much less than that in our study. Considering there so many Cu-related defects inside the CIS NCs, some Zn^{2+} may fill the vacancy sites related to Cu-defects in the process of introducing Zn into CIS. In combination with cation exchange, Zn interstitials at Cu vacancy sites will result in the introduction of more Zn^{2+} into CIS NCs, meaning much more ZnS being incorporated into CIS which naturally increases the level of blue-shift. The higher the diffusion temperature, the higher the reactivity of Zn^{2+}, and the more the amount of Zn^{2+}. Therefore, the broad PL spectra are attributed to both partial cation exchange and the filling of vacancy sites related to Cu-defects, the latter of which may play a more important role.

To further improve the PLQY, the surface passivation was made by in situ growth of a ZnS shell on the CIZS core NCs. As shown in Fig. S2, a dramatic improvement on PLQY could be viewed for all the CIZS NCs (a range of 45–76%) after the ZnS overcoating due to the elimination of surface trap states. From the HRTEM image in Fig. S3, the sizes of CIZS/ZnS NCs are about 3.1 nm, slightly larger than those of the plain CIZS core NCs, indicating the successful growth of ZnS shell on the CIZS core NCs.

PL relaxations of CIS, CIZS and CIZS/ZnS NCs were characterized, which could be well fitted by a triple-exponential function: $I(t)=A_1\exp(-t/\tau_1)+A_2\exp(-t/\tau_2)+A_3\exp(-t/\tau_3)$ [14]. As shown in Fig. 4, CIS NCs exhibit a more rapid decay of photoluminescence which is attributed to nonradiative recombination induced by the intrinsic and surface defects [10]. In contrast, the contribution of fast decay components τ_1 and τ_2 decreased while long decay component τ_3 increased for the CIZS NCs (Table S3), indicating that the amount of structural defects was reduced by the diffusion of Zn into CIS crystal structure, and thus inducing a suppressed nonradiative recombination process. However, due to the alloyed structure rather than the core/shell structure, the surface defects could not be completely eliminated, which led to the fact that contribution of τ_2 related to surface states is not reduced effectively and the PL decay curve of CIZS is only modified to some extent but still remains triple-exponential. After ZnS coating, the fast decay components τ_1 and τ_2 were highly suppressed and simultaneously the average lifetime was extended to 274.1 ns. In addition, the decay profile appeared to be almost uniformly single-exponential, indicating the complete elimination of surface defects and a single highly emissive recombination channel across the entire NC ensemble, which could be correlated to the dramatic improvement in PLQY and stability (Fig. S4).

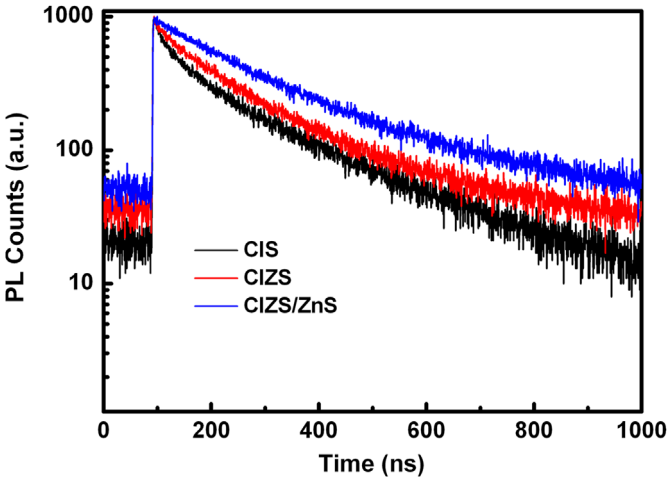

Fig. 4. PL lifetime decays of CIS, CIZS and CIZS/ZnS NCs.

4. Conclusion

In summary, we reported the synthesis of Cu–In–Zn–S alloyed nanocrystals through a facile solution method. By adjusting diffusion temperature, the CIZS NCs exhibited broad PL spectra with tunable emission colors from visible to NIR regions. The resulting NCs were nearly spherical and had narrow size distribution. After the deposition of ZnS shell, the PLQY increased substantially with a maximum value of 76%. The single exponential PL decay with an increased average lifetime suggested a suppressed nonradiative recombination process related to structural defects. Therefore, the obtained NCs exhibit promising applications in cell imaging, LEDs and solid-state lighting.

Acknowledgments

This research was supported by the National Natural Science Foundation of China (21175051) and Fundamental Research Funds for the Central Universities (2013SC17).

Appendix A. Supporting information

Supplementary data associated with this article can be found in the online version at http://dx.doi.org/10.1016/j.matlet.2013.12.109.

References

[1] Li L, Pandey A, Werder DJ, Khanal BP, Pietryga JM, Klimov VI. J Am Chem Soc 2011;133:1176–9.
[2] Chen BK, Zhong HZ, Wang MX, Liu RB, Zou BS. Nanoscale 2013;5:3514.
[3] Nam DE, Song WS, Yang HS. J Colloid Interface Sci 2011;361:491–6.
[4] Nakamura H, Kato W, Uehara M, Nose K, Omata T, Maeda H, et al. Chem Mater 2006;18:3330–5.
[5] Zhang J, Xie RG, Yang WS. Chem Mater 2011;23:3357–61.
[6] Chen BK, Zhong HZ, Zhang WQ, Tan ZA, Li YF, Yu CR, et al. Adv Funct Mater 2012;22:2081–8.
[7] Zhang WJ, Zhong XH. Inorg Chem 2011;50:4065–72.
[8] Tang XS, Ho WBA, Xue JM. J Phys Chem C 2012;116:9769–73.
[9] Li L, Daou TJ, Texier I, Kim TT, Liem NQ, Reiss P. Chem Mater 2009;21:2422–9.
[10] Zhong HZ, Bai ZL, Zou BS. J Phys Chem Lett 2012;3:3167–75.
[11] Tang XS, Cheng WL, Choo ESG, Xue JM. Chem Commun 2011;47:5217.
[12] Park J, Kim SW. J Mater Chem 2011;21:3745.
[13] De Trizio L, Prato M, Genovese A, Casu A, Povia M, Simonutti R, et al. Chem Mater 2012;24:2400–6.
[14] Zhong HZ, Zhou Y, Ye MF, He YJ, Ye JP, He C, et al. Chem Mater 2008;20:6434–43.